Automatic Mesh Optimization of Direct Simulation Monte Carlo Methods for Hypersonic Flows

Shrutakeerti M.V.[1], Vincent Casseau[2], and Wagdi G. Habashi[3]
CFD Laboratory, McGill University, Montreal, QC, H3A 2S6, Canada

Abolfazl Karchani[4]
Ansys, Inc., Lebanon, NH, 03766, USA

I. Introduction

The Direct Simulation Monte Carlo (DSMC) method is a particle-based probabilistic method widely used to solve the Boltzmann transport equation (BTE). The development and testing of a sophisticated DSMC code is part of an ongoing effort to build a multi-physics simulation tool to be used in the design process of a High-Altitude Low Orbit (HALO3D) civil transport vehicle. This is a multidisciplinary undertaking to tackle physical phenomena in hypersonic flows such as thermochemical non-equilibrium and magnetohydrodynamic effects. The low-altitude flow field is obtained with an edge-based unstructured FE Navier–Stokes (HALO3D-NS) portion of the code for the continuum and continuum-transition regimes [1, 2] where the linear constitutive relations for shear stress and heat flux hold true. At higher altitudes, for large departures from local thermal equilibrium (LTE), a DSMC (HALO3D-DSMC) solver is required to account for the nonequilibrium phenomena. Hence, the seamless simulation of the entire flight envelope of a hypersonic vehicle requires codes able to simulate the atmosphere as a continuum or as a particulate medium, either independently from each other or jointly when appropriate. The simulation of such multiscale fluid structures and thermochemistry should greatly benefit the use of a common automated mesh optimization method to fully resolve the corresponding terms of the NS and BTE equations.

Mesh optimization for DSMC, as clearly shown for NS [2], ought to improve the solution accuracy and help minimize the statistical fluctuations inherent in the calculation of cell-based averages by ensuring that the cell characteristic size converges to the order of the local mean free path in the regions of interest. Along with this, mesh optimization should better capture salient flow features such as shocks, expansion fans, recirculation zones and boundary layers. The mesh optimization method, OptiGrid [3], used in the NS portion of HALO3D involves a combination of mesh operations driven by an error estimate based on the Hessian of a single variable or combination of variables of the PDE.

One of the early works on mesh refinement for DSMC is the Adaptive Mesh and Algorithm Refinement (AMAR) technique of Garcia *et al*. [4]. Here, mesh adaptation is performed for a hybrid NS-DSMC algorithm with a block structured hierarchical refinement strategy for the spatial domain and an adaptive time step algorithm for the temporal domain which advances different levels of the mesh at different rates based on CFL considerations. There are two main approaches to mesh optimization for DSMC – an unstructured mesh based approach [5-8] and a Cartesian/octree mesh based approach. Cartesian/octree methods are categorized into n-level Cartesian mesh [9-12] and recursive Adaptive Mesh Refinement (AMR) techniques [13-16]. The choice of an optimization scalar to compute an error norm to refine or coarsen the mesh is crucial. Many of the Cartesian techniques [7-10, 12-15] compute the local mean free path (mfp) and directly refine the cells whose dimensions are greater than the local mfp. While local mfp sets an upper limit to the allowable cell size, a lower limit to the allowable cell size can be applied when considering that excessively

[1] Doctoral Student, CFD Laboratory Department of Mechanical Engineering, 680 Sherbrooke St. West shrutakeerti.mallikarjun@cfdlab.mcgill.ca
[2] Postdoctoral Researcher, CFD Laboratory Department of Mechanical Engineering, 680 Sherbrooke St. West
[3] Professor and Director, CFD Laboratory Department of Mechanical Engineering, 680 Sherbrooke St. West
[4] Senior Research & Development Engineer, ANSYS, 10 Cavendish Ct

refined patches of the mesh will register low particle counts which in turn will cause the macroscopic averages to deteriorate. In order to rectify this, some techniques [14] are able to enforce a number of particles constraint while refining – the cell is not refined if the number of particles in the cell is less than or equal to a threshold number. In unstructured mesh and some Cartesian mesh methods, density [5] and the gradients of density and velocity [6, 9, 13, 15] have been used as optimization scalars. The ease of generating the mesh in the regions of interest, flexibility in mesh adaptation and ability to accommodate complex geometry lets Wu *et al*. [5] conclude that unstructured mesh approaches are superior to structured mesh approaches. Flows over a cylinder [5, 8, 13], leading edge [6] and wedge [13, 14, 15], among others, are used as verification test cases in the literature. The codes are then applied to real geometries such as a scramjet configuration [8], reentry vehicles [13], the Hubble space telescope [11], planetary probes [7, 10, 12] and the space shuttle [11].

A stochastic method such as DSMC produces macroscopic averages that are prone to statistical scatter or noise. Sampling error in DSMC arises from the use of finite N_s samples to obtain the final macroscopic averages. Error is also introduced from the approximation of W_p molecules with one particle, or by using too small a number of particles, N_p. Using too large a time step that is not of the order of the local mean collision time or using too large collision cells that are not on the order of the local mean free path also contributes to error. While the best way to deal with sampling error is to employ good DSMC practices, other methods can be used in conjunction to treat statistical scatter. Kaplan *et al*. [17] use Flux Corrected Transport (FCT) filtering as a postprocessing tool to reduce the scatter in their charged species number density fields for the ionized Mach 44 flow around the Stardust capsule. Cave *et al*. [18] use the DSMC Rapid Ensemble Averaging Method (DREAM) to reduce scatter. DREAM uses a combination of time averaged data and ensemble averaged macroscopic data to obtain low scatter solutions for the interaction of a Mach 4 shock wave with a square cavity and a Mach 12 shock impingement over a wedge in a channel. Along with these, DSMC Information Preservation (IP) methods have been developed [19] to reduce statistical scatter by preserving macroscopic field data with each particle in addition to the particles' microscopic data.

The attributes of some well-known DSMC – mesh optimization codes are now discussed. The SMILE [9] DSMC code uses a two-layer rectilinear adaptive mesh for collision modeling. One layer is needed for particle tracking and to calculate the majorant collision frequency. The other layer is used to group particles together for collision operations. Mesh adaptation is performed on the collisional grid. NASA's DSMC Analysis Code (DAC) [11] employs separate meshes for the flowfield and the surface, with the flowfield grid being a two-level Cartesian mesh and the surface mesh being an unstructured triangular mesh. DAC first creates an initial coarse mesh with cells the size of the freestream mfp. Following this, either the local flow gradients or the mfp requirement dictate the refinement in the domain. MONACO [7] employs an unstructured tetrahedral mesh and refines the mesh based on local mfp. The Molecular Gas Dynamics Simulator (MGDS) [12] employs a three-level Cartesian grid for the flowfield. The third level of refinement offers considerable flexibility over two-level implementations for flows with large gradients. OpenFOAM's DSMC solver, dsmcFOAM [15], utilizes a structured mesh with AMR capabilities. Sandia National Lab's SPARTA [16] code utilizes a 2D/3D hierarchical Cartesian mesh. The topmost level of the mesh is the simulation box and each parent cell can have as many child cells in each direction. As many levels as needed can be created recursively.

II. Methodology

A. HALO3D-DSMC

The background grid employed to localize particles for the collision step is an unstructured grid composed of finite element primitive cells. Macroscopic averages are calculated for the specified number of samples in the cells of the background collisional grid. Following this, an inverse distance weighted interpolation method is used to interpolate cell centered macroscopic averages at the nodes. The algorithm of Macpherson *et al.* [20] is used for particle tracking because it can be employed on unstructured polyhedral meshes and has proven to be robust. Here, built in finite element cell-facet-node connectivity data is used in a facet-intersection based tracking routine. An a-priori estimate of the number of collisions to occur in the collision step is provided by the No-Time-Counter (NTC) algorithm [21]. This is one of the most widely used collision schemes and it requires at least 20 particles in each collision cell. In this paper, collisions are deemed to be inelastic and are described by the Variable Hard Sphere (VHS) model [22]. Energy redistribution between the translational and rotational energy modes is computed according to the standard Larsen–Borgnakke (LB) procedure [23] involving a constant rotational collision number whose value is usually taken equal to 5. Finally, the post-collision rotational energy is sampled from an equilibrium distribution that is parameterized on the collision energy [22]. The macroscopic averages obtained using DSMC are ergodic in nature and can be calculated

by either taking a time average or an ensemble average over several independent ensembles. Independence between each ensemble is guaranteed by providing a different random number seed to each ensemble's random number generator. All the results presented in this study have used 2-6 ensembles.

B. OptiGrid

OptiGrid, developed by the McGill CFD lab and now distributed by ANSYS, generates meshes that are tailor made to homogenize the error everywhere with much less mesh points than blind refinement based on gradients, greatly reducing the meshing and computational effort and significantly increasing solution accuracy. OptiGrid has been used with finite volume and finite element solvers and has been shown to yield the same final mesh [3] for both approaches, and it is believed to be the first time that it is being adapted to a particle method. OptiGrid operates on any mesh to equalize and minimize the interpolation error through four basic mesh operations driven by an error estimate given in eq. 2. These constitute three binary operations: edge refinement, edge coarsening and edge swapping and one continuous operation: node movement. The binary operations are either "on" or "off" operations and node movement models the edges surrounding the node to be moved as springs. The stiffness constant of the springs is proportional to the edge error estimate. These operations are shown in fig. 1

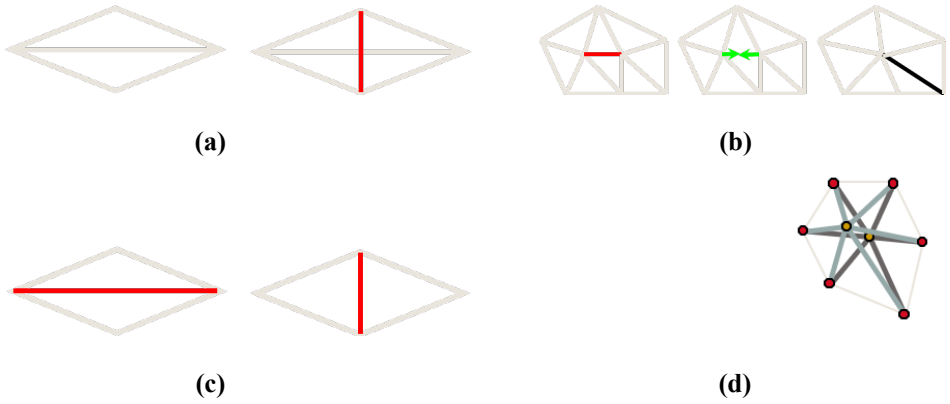

Figure 1. a) refinement b) coarsening c) swapping d) movement

The optimization algorithm requires firstly a scalar such as density, directional velocity, temperature or number of particles. The Hessian, $\boldsymbol{H}$ of the scalar is computed and decomposed as in eq. 1 The edge based error estimate is the computed from eq. 2 An optimization target needs to be specified as either a prescribed error level or a certain number of nodes and cells. The constraints for optimization are the minimum and maximum allowed edge lengths and maximum aspect ratio of the cells.

$$\boldsymbol{H} = \boldsymbol{R}\boldsymbol{\Lambda}\boldsymbol{R}^{\boldsymbol{T}} \qquad \boldsymbol{M} = \boldsymbol{R}|\boldsymbol{\Lambda}|\boldsymbol{R}^{\boldsymbol{T}} \tag{1}$$

$$\mathbf{e}(\boldsymbol{x_i} - \boldsymbol{x_j}) = \int_0^1 \sqrt{(\boldsymbol{x_i} - \boldsymbol{x_j})^T \boldsymbol{M}(\boldsymbol{l})(\boldsymbol{x_i} - \boldsymbol{x_j})}\, \boldsymbol{dl} \tag{2}$$

III. Results

A. Bird's leading edge case

The canonical leading edge test case is commonly used to verify DSMC codes. This is a 2D test case of the Mach 4 flow of molecular nitrogen over a diffuse wall. The results from the structured grid used by Bird [22] are used as a baseline to compare the results of adapted meshes. The freestream pressure is 0.4142 Pa, freestream temperature is 300 K, freestream x-velocity is 1412.5 m/s, wall temperature is 500 K, number of samples is 20,000, number of simulators is 350,000 and timestep is 2e-6 s. The optimization scalar set is (ρ T_t T_r P U_x U_y), where ρ is the mixture density, T_t is the translational temperature, T_r is the rotational temperature, P is the pressure, U_x is the velocity in the

x-direction and U_y is the velocity in the y-direction. The optimization target is 5000 nodes with the maximum threshold on the number of elements being 15,000. The minimum edge length is set to be equal to the stagnation point mean free path. The adapted grid shown in fig. 2 captures the shock well and has adequate refinement near the wall.

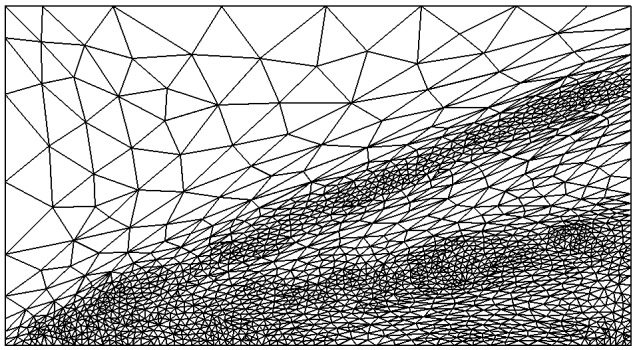

Figure 2. Mesh optimized with the scalar set ($\rho, T_t, T_r, P, U_x, U_y$) used to calculate the error estimator

The contours of mean collision separation (mcs) by mean free path (mfp) in fig. 3 show that mcs/mfp is less than 1 in the regions of interest like the shock and boundary layer. Plots of surface heat flux and shear stress in fig. 4 compare well with structured grid results.

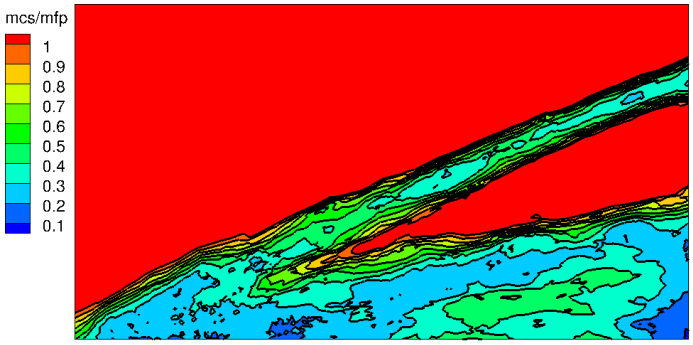

Figure 3. mcs/mfp for the leading edge

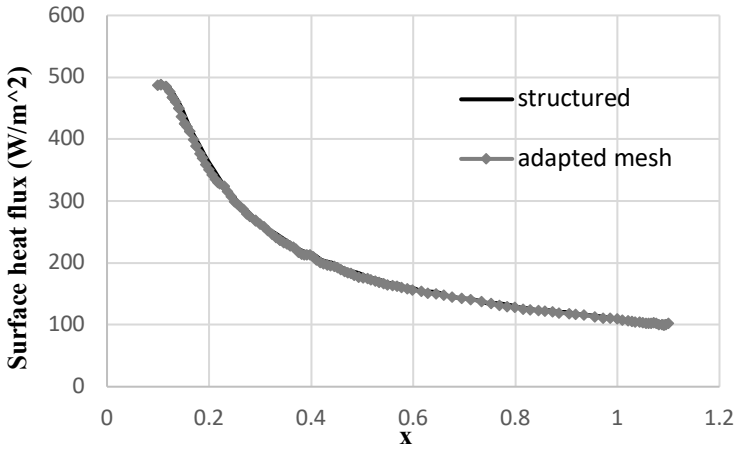

Figure 4. Surface heat flux for the structured and adapted meshes

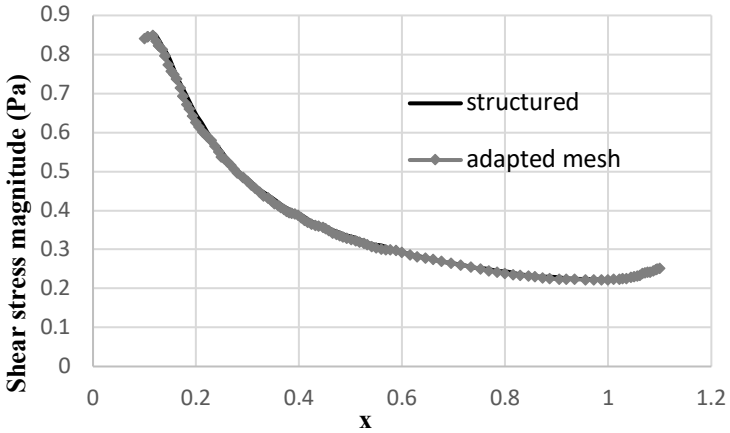

Figure 5. Shear stress for the structured mesh and adapted meshes

B. Bird's supersonic corner case

The supersonic corner [22] is the 3D analogue of the 2D leading edge. This is a Mach 6 flow of Argon over a diffuse wall corner. A patch of specular wall is present upstream of the diffuse wall. The freestream pressure is 0.41419 Pa, freestream temperature is 300 K, freestream x-velocity is 1936 m/s, wall temperature is 1000 K, number of samples is 30,000, particle weight is 2e12, timestep is 1e-6 s. The optimization scalar is ($\rho\ T_t\ T_r\ P\ U_x\ U_y\ U_z$) and the optimization target is 20,000 nodes with the maximum threshold on the number of elements being 70,000. The adapted mesh is shown in fig. 5 where the freestream cells are coarse and the mesh distribution on the wall is refined.

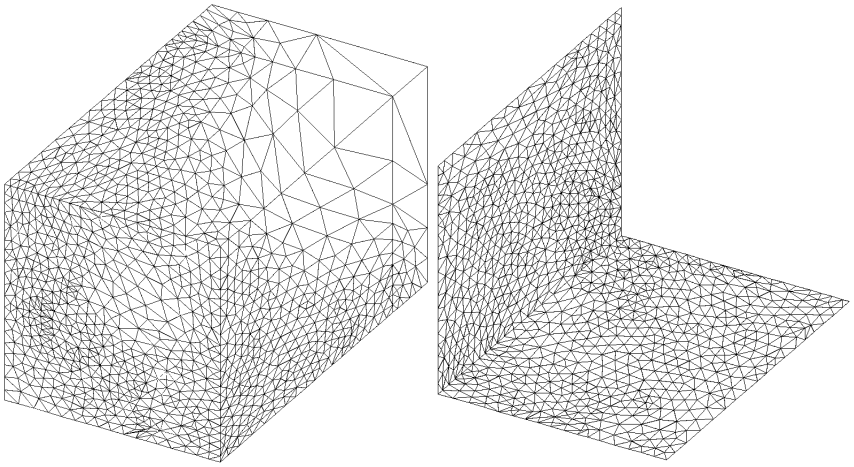

Figure 6. Optimized mesh for the supersonic corner

Contours of mcs/mfp show that the ratio is less than 1 in nearly all of the domain, hence guaranteeing correct selection of collision candidates. Contours of shear stress magnitude and surface heat flux are presented in fig. 7 and 8, both of which, agree with the structured mesh solutions.

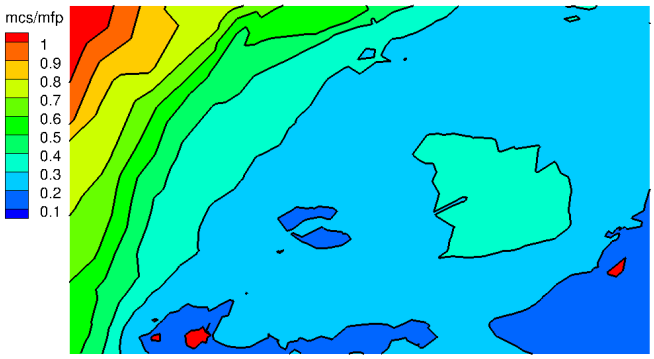

Figure 7. mcs/mfp for the supersonic corner

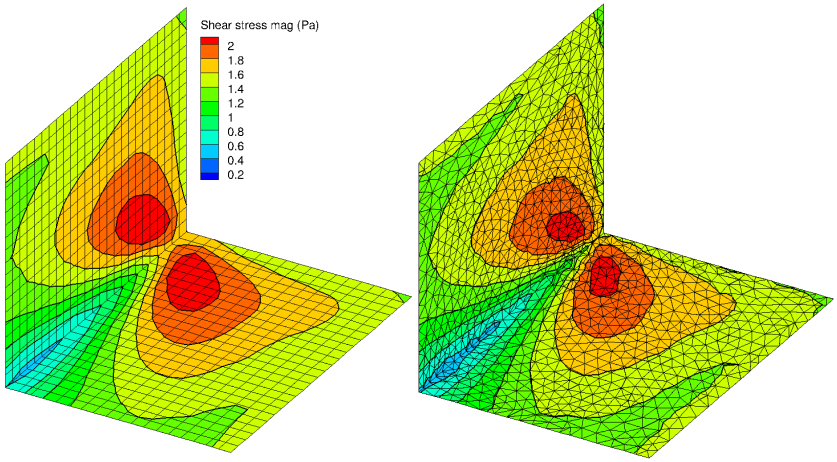

Figure 8. Shear stress magnitude for the structured mesh and the optimized mesh

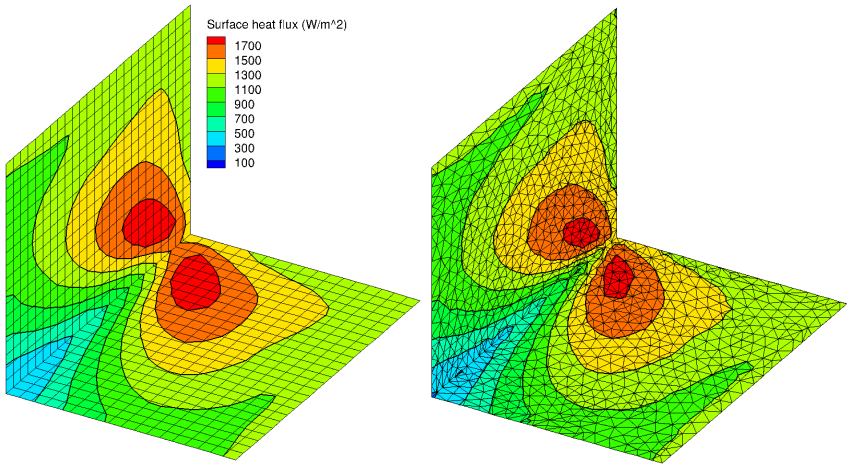

Figure 9. Surface heat flux for the structured mesh and optimized mesh

IV. Conclusions and future work

This study presents the application of a Hessian based mesh optimization algorithm, OptiGrid, to a DSMC code, HALO3D-DSMC. Two test cases are used in this investigation: the supersonic leading edge and the supersonic corner

flow. Results from structured grids are used as a baseline to compare against the results from mesh optimization. The optimization scalar set ($\rho\ T_t\ T_r\ P\ U_x\ U_y$) is found to be good at predicting surface quantities such as the heat flux and shear stress. The optimized grid captures the shock and the region near the wall is appropriately refined. Following the leading edge case, the optimization scalar set for the supersonic corner is chosen to be ($\rho\ T_t\ T_r\ P\ U_x\ U_y\ U_z$). Contours of shear stress and heat flux are shown to agree reasonably between the structured and optimized meshes. Continuing this work can be accomplished in the following areas. Mesh optimization with the optimization target being the number of elements can be investigated. More parameters such as Mach number can be used as optimization scalars. More complex flows such as over a cylinder or a capsule can be simulated.

Acknowledgements

The CFD Lab extends its thanks to the Lockheed Martin Corporation, Ansys Inc and MITACS for the MITACS Accelerate grant supporting the current work.

References

[1] Seguin, J., Gao, S., Habashi, W.G., Isola, D., and Baruzzi, G.S., "A finite element solver for hypersonic flows in thermo-chemical non-equilibrium, Part I", *Invited Paper to Special Issue of the International Journal of Numerical Methods in Heat and Fluid Flow*, Vol. 29, No. 7, 2019, pp. 2352-2388.

[2] Seguin, J., Gao, S., Habashi, W.G., Isola, D., and Baruzzi, G.S., "A finite element solver for hypersonic flows in thermo-chemical non-equilibrium, Part II", *Invited Paper to Special Issue of the International Journal of Numerical Methods in Heat and Fluid Flow*, Vol. 30, No. 2, 2020, pp. 575-606.

[3] Habashi, W.G., Dompierre, J., Bourgault, Y., Fortin, M., and Vallet, M.G., "Certifiable Computational Fluid Dynamics Through Mesh Optimization, Special Issue on Credible Computational Fluid Dynamics Simulation", *AIAA Journal*, Vol. 36, No. 5, 1998, pp. 703-711.

[4] Garcia, A.L., Bell, J.B., Crutchfield, W.Y., and Alder, B.J., "Adaptive Mesh and Algorithm Refinement Using Direct Simulation Monte Carlo", *Journal of Computational Physics*, Vol. 154, No. 1, 1999, pp. 134-155.

[5] Wu, J.S., Tseng, K.C., and Kuo, C.H., "The direct simulation Monte Carlo method using unstructured adaptive mesh and its application", *International Journal for Numerical Methods in Fluids*, Vol. 38, No. 4, 2002, pp. 351-375.

[6] Kim, M.G., Hyoung S.K., and Oh J.K., "A parallel cell-based DSMC method on unstructured adaptive meshes", *International Journal for Numerical Methods in Fluids*, Vol. 44, No. 12, 2004, pp. 1317-1335.

[7] Dietrich, S. and Boyd, I.D., "Scalar and Parallel Optimized Implementation of the Direct Simulation Monte Carlo Method", *Journal of Computational Physics*, Vol. 126, No. 1, 1996, pp. 328-342.

[8] Su, C.C., Tseng, K.C., Wu, J.S., Cave, H.M., Jermy, M.C., and Lian, Y.Y., "Two-level virtual mesh refinement algorithm in a parallelized DSMC Code using unstructured grids", *Computers & Fluids*, Vol. 48, No. 1, 2011, pp. 113-124.

[9] Ivanov, M.S., Kashkovsky, A.V., Gimelshein, S.F., Markelov, G.N., Alexeenko, A.A., Bondar, Y.A., Zhukova, G.A., Nikiforov, S.B., and Vaschenkov, P.V., "SMILE system for 2D/3D DSMC computations", *Proceedings of 25th International Symposium on Rarefied Gas Dynamics, St. Petersburg, Russia*, 2006, pp. 21-28.

[10] Nompelis, I. and Schwartzentruber T.E., "Strategies for Parallelization of the DSMC Method", AIAA Paper 2013-1204, in *51st AIAA Aerospace Sciences*, 2013.

[11] LeBeau, G.J. and Lumpkin III, F.E., "Application highlights of the DSMC Analysis Code (DAC) software for simulating rarefied flows", *Computer Methods in Applied Mechanics and Engineering*, Vol. 191, No. 6, 2001, pp. 595-609.

[12] Gao, D., Zhang, C., and Schwartzentruber, T.E., "Particle Simulations of Planetary Probe Flows Employing Automated Mesh Refinement", *Journal of Spacecraft and Rockets*, Vol. 48, No. 3, 2011, pp. 397-405.

[13] Arslanbekov, R., Kolobov, V., Burt, J., and Josyula, E., "Direct simulation Monte Carlo with octree Cartesian mesh", AIAA Paper 2012-2990, in *43rd AIAA Thermophysics Conference*, 2012.

[14] Sawant, S.S., Tumuklu, O., Jambunathan, R., and Levin, D.A., "Application of adaptively refined unstructured grids in DSMC to shock wave simulations", *Computers & Fluids*, Vol. 170, No. 1, 2018, pp. 197-212.

[15] White, C., "Adaptive Mesh Refinement for an Open Source DSMC Solver", AIAA Paper 2015-3632, in *20th AIAA International Space Planes and Hypersonic Systems and Technologies Conference*, 2015.

[16] Klothakis, A.G., Nikolos, I.K., Koehler, T.P., Gallis, M.A., and Plimpton, S.J., "Validation simulations of the DSMC code SPARTA", *AIP Conference Proceedings*, Vol. 1786, No. 1, 2016, p. 050016.

[17] Kaplan, C.R., Oran, E., and Aggarwal, U., "Reducing statistical scatter in DSMC solutions of hypersonic ionizing flows", AIAA Paper 2016-3843, in *46th AIAA Thermophysics Conference*, 2016.
[18] Cave, H.M., Jermy, M.C., Tseng, K.C., and Wu, J.S., "DREAM: An Efficient Methodology for DSMC Simulation of Unsteady Processes", *AIP Conference Proceedings*, Vol. 1084, No. 1, 2008, pp. 335-340.
[19] Cai, C., Boyd, I.D., Fan, J., and Candler, G.V., "Direct simulation methods for low-speed microchannel flows", *Journal of Thermophysics and Heat Transfer*, Vol. 14, No. 3, 2000, pp. 368-378.
[20] Macpherson, G.B., Nordin, N., and Weller, H.G., "Particle tracking in unstructured, arbitrary polyhedral meshes for use in CFD and molecular dynamics", *Communications in Numerical Methods in Engineering*, Vol. 25, No. 1, 2009, pp. 263-273.
[21] Bird, G.A., "Perception of Numerical Methods in Rarefied Gasdynamics", *Progress in Astronautics and Aeronautics*, Vol. 117, 1989, pp. 211-226.
[22] Bird, G.A., "Molecular Gas Dynamics and the Direct Simulation of Gas Flows", *Clarendon Press,* 1994.
[23] Borgnakke, C. and Larsen, P.S., "Statistical collision model for Monte Carlo simulation of polyatomic gas mixture", *Journal of Computational Physics*, Vol. 18, No. 4, 1975, pp. 405-420.